

ANALYSIS OF TIME-DEPENDENT LOSS MODELS FOR SEGMENTAL BRIDGES

George Tsiatas, PhD, Dept. of Civil Engineering, University of Rhode Island
Everett McEwen, PhD, Dept. of Civil Engineering, University of Rhode Island
Silvia Essmann, Grad. Student, Dept. of Civil Engineering, Univ. of Rhode Island

ABSTRACT

A nonlinear, time-dependent analysis of a segmental post-tensioned bridge is carried out to evaluate concrete strains at the mid-span closure segment. The American Concrete Institute (ACI) and European (CEB) approaches for modeling time dependent material behavior are considered and the rate of creep method is used to account for moment redistribution. The strains calculated are compared with strains monitored using embedded Carlson strain meters.

Applying the prediction method provided by the CEB MC 90, calculated strains are in good agreement with the monitored strains. On the other hand, calculated strains using the ACI approach are larger than the monitored strains.

Keywords: Bridges, Segmental Bridges, Creep, Shrinkage, Prestress Losses.

INTRODUCTION

Segmental concrete construction has become popular for medium and long span bridges in North America since the 1970s. One of the design problems for such bridges is the time dependency of various properties including creep and shrinkage effects. Time dependent effects are very important especially in cast-in-place cantilever constructions because deformation and prestress losses take place during the whole period of construction, and hence, the exact construction sequence has to be followed for the analysis. Furthermore, a change in the statical system takes place when the cantilever components are connected to form a continuous system. This leads to time-dependent moment redistributions due to creep. In order to verify design procedures and expand the knowledge of the time varying effects on segmental bridges, a monitoring program of the newly built Jamestown-Verrazano bridge was undertaken.

The Jamestown-Verrazano Bridge is a partially cast-in-place, cantilever constructed, post-tensioned, concrete box girder bridge located over the Narragansett Bay in Rhode Island. Construction of the bridge finished in 1992. The main span closure segment as well as a segment adjacent to one of the piers of the main structure was instrumented with thermocouples and strain meters during construction to monitor temperatures and longitudinal strains in the bridge¹.

In the present study the focus is on the longitudinal strains. The purpose is to compare calculated time-dependent strains, using existing theories, with monitored strains in the main span closure segment. Calculations are made using the Rate of Creep Method. The necessary time-dependent concrete properties are determined according to the ACI 209 prediction method and the method provided by the CEB-FIP MC 90. To obtain forces and moments, a computer model of the segmentally constructed box girder bridge is used. Prestress losses and strains are determined using a spreadsheet. The construction history of the bridge is taken into consideration. The Jamestown-Verrazano Bridge provides a unique opportunity to obtain information on the time dependent behavior of a cast-in-place segmental concrete box girder bridge for the New England area.

BRIDGE GEOMETRY AND STRAIN MONITORING PROGRAM

The Jamestown-Verrazano Bridge is located over the Narragansett Bay to the south of Providence, Rhode Island. The total length of the bridge is 7,350 ft with a main span navigational clearance of 600 ft in horizontal and 135 ft in vertical direction. The roadway width of the bridge is 74 ft and supports two lanes of traffic in each direction. The bridge is made up of 52 spans, 29 of which comprise the approach spans and the remaining 23 are the main structure. Eleven spans of the main structure form the west approach, nine spans form the east approach and the remaining three comprise the main span section. It is the main

span section which is the focus of the present study, Fig. 1. This consists of three spans made from a double-cell, post tensioned concrete box girder built by the balanced cantilever, cast-in-place, technique. The center span is 674 ft long and the two side spans are 359 ft long each. The depth of the box girder changes from 10 ft at the main span closure to 30 ft 10 in at the pier supports.

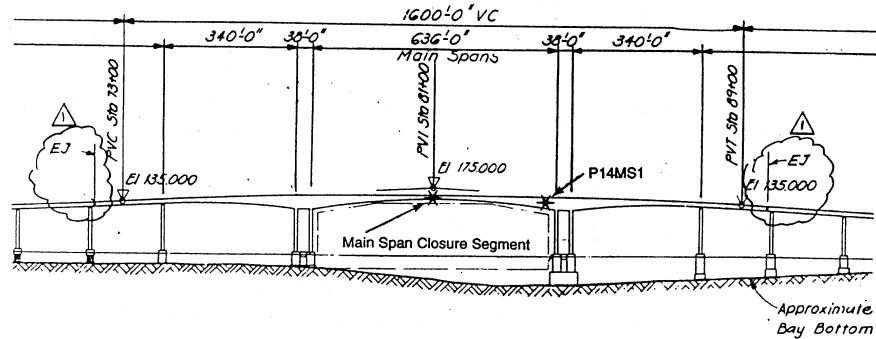


Fig. 1 Main Span Section¹

During instrumentation of the bridge eight strain sensors were installed into the main span closure segment. These are Carlson strain meters type A-10 with 4 wire conductor cables and are capable of measuring concrete strains as well as concrete temperatures at the location of the meters. Four of the sensors (#1 through #4) were placed in the formwork prior to concrete casting and four were placed by retrofitting at the same locations as the embedded strain meters (#5 though #6). The location of the strain meters in the main span closure segment is demonstrated in Fig. 2.

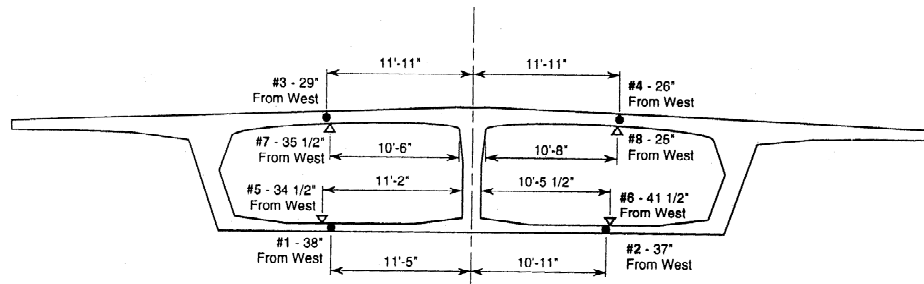


Fig. 2 Location of Strain Meters in Main Span Closure Segment

All strain readings are temperature adjusted to a reference temperature of 73°F. Data were originally read manually but an Automated Data Acquisition System (ADAS) was later installed for continuous monitoring², Fig. 3.

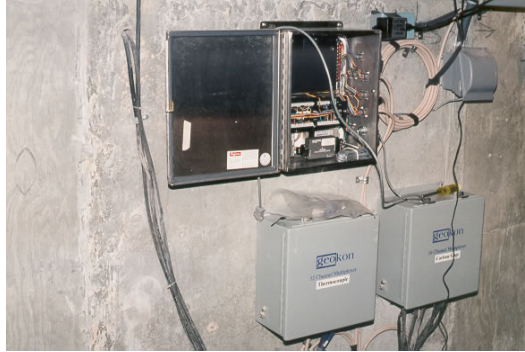


Fig. 3 ADAS

MAIN SPAN CONSTRUCTION

The construction sequence is summarized here since it is important for the time-dependent analysis of the bridge. The main span was constructed using the cantilever construction method with a profile shown in Fig. 4. The pier tables, constructed above the shafts of Piers 13 and 14, became the initial segments. From Pier 13 and Pier 14, the cantilever main span extends approximately 300 feet in each direction before joining in the center (Span 13) and closing with the East and West Approaches at Piers 15 and 12. The pier tables were cast-in-place and measure approximately 60 feet in length and 33 feet in depth. While the exterior of the pier tables resembles a pier segment with the exception of the larger depth, it internally differs from the standard pier segments. Because of the later post-tensioning of the main span, a large quantity of embedded ducts and tubes with high strength steel cables were placed in the pier table. A total of 91 ducts were installed.

Twenty one segments were constructed on each side of piers 13 and 14. The segments on the main span side of the cantilever were cast first, and at least one cantilever tendon was stressed. Afterwards, the corresponding segment on the side span side of the cantilever was cast and the remaining cantilever tendons were stressed. After finishing the cantilever segments, the closure segments connecting the cantilever structure to the approach spans were cast, and the continuity tendons in the side spans were stressed. The continuity tendons in the side spans consist of a total of 12 27x0.5" diameter tendons in each span. Prior to casting the main span closure segment, the bridge cantilevers were jacked apart applying a

force of 800 kips. A few days afterwards, the main span closure segment was cast and stressed. Stressing took place within a period of 12 days. A total of 16 31x0.5" diameter tendons were used.

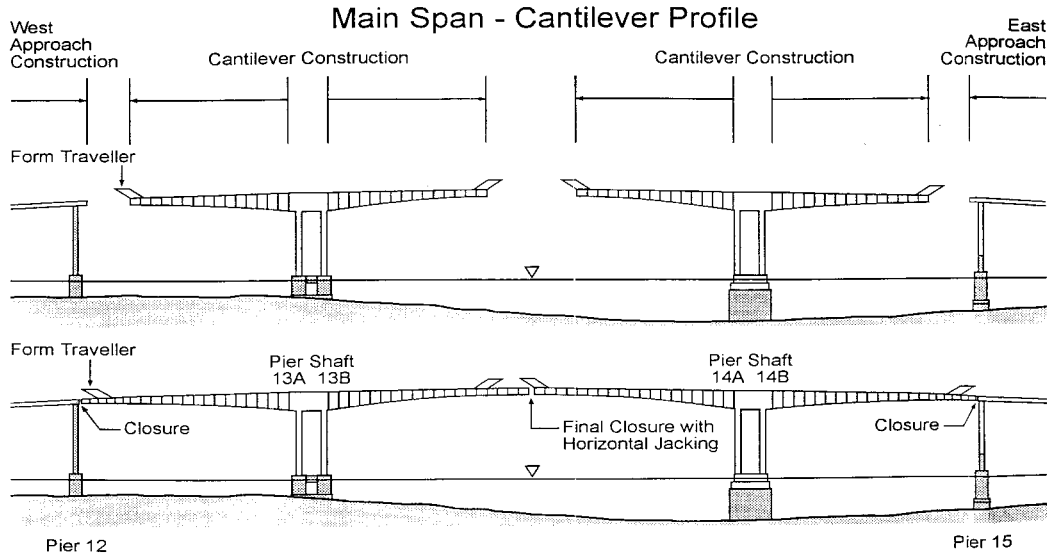


Fig. 4 Main Span Cantilever Profile

TIME DEPENDENT MATERIAL PROPERTIES

There are several approaches to incorporate the time variation of concrete creep and shrinkage. In order to select the approach to be used, concrete creep and shrinkage strains obtained from experimental test data were compared to standard prediction methods established by ACI (ACI 209) and two European specifications, namely the Improved CEB-FIP MC 78 specification and the CEB-FIP 90 code. The measured shrinkage strains agree well with the ACI 209 predictions. The two European model codes predict shrinkage strains that are close to each other but lower than the measured and the ACI results. The opposite is true for the case of the creep strains where ACI 209 results are lower than the measured creep whereas the CEB 90 and CEB 78 results are comparable to the measurements. However, the total strains, i.e. both shrinkage and creep strains considered together are comparable for all cases³.

Based on the results of the comparative study, the methods provided by Committee 209 of the American Concrete Institute (ACI 209R-92) and those of the Comité Euro-International Du Béton (CEB-FIP Model Code 1990) are used here to model the time dependent behavior of concrete.

ACI 209R-92

A simplified approach for determining creep factors and shrinkage strains is used by the ACI 209R-92⁴. For the case of the Jamestown-Verrazzano bridge the equations for determining the shrinkage strain and the creep coefficient are given as follows

$$(\varepsilon_{sh})_{t-t_s} = 901 \times 10^{-6} \frac{t-t_s}{35+(t-t_s)} \quad (1)$$

$$\nu_t = 2.413 \frac{t^{0.6}}{10+t^{0.6}} \quad (2)$$

where t_s is the age of concrete in days when shrinkage starts, typically immediately after the initial wet curing. In this case $t_s=1$. The coefficients in Equations 1 and 2 have been determined considering the age of the concrete at the time of loading (3 days), the initial moist cure, the relative humidity, the average thickness of the structural member, and the concrete composition.

The time-dependent modulus of elasticity of the concrete is also needed for creep calculations at different times of loading, especially when concrete is loaded at a young age. According to ACI and for the type of materials and curing methods followed in this bridge the equation for predicting the time-dependent compressive strength of concrete is given as:

$$(f_c')_t = \frac{t}{4+0.85t} (f_c')_{28} \quad \text{for } t < 28 \text{ days} \quad (3)$$

$$(f_c')_t = (f_c')_{28} \quad \text{for } t \geq 28 \text{ days} \quad (4)$$

Then, the time-dependent modulus of elasticity of the concrete can be determined as follows:

$$E_{ct} = 33w^{1.5} \sqrt{(f_c')_t} \quad (5)$$

where w is the unit weight of concrete in pcf and t is the age of concrete in days.

CEB-FIP MC 90

According to the CEB-FIP Model Code 1990⁵ and considering the mean compressive strength of concrete at 28 days, the type of cement, the relative humidity and other factors the expression for the shrinkage strain is given as:

$$\varepsilon_{cs}(t, t_s, t_0) = 532.28 \left[\left(\frac{t-t_s}{203.23+t-t_s} \right)^{0.5} - \left(\frac{t_0-t_s}{203.23+t_0-t_s} \right)^{0.5} \right] \quad (6)$$

where t = age of concrete in days,

t_s = age of concrete at the beginning of shrinkage, which is the end of wet curing.

t_0 = age of concrete at the time from when shrinkage is considered.

For predicting the creep coefficient, the following equation is provided in the CEB-FIP MC 90:

$$\Phi(t, t_0) = \Phi_0 \beta_c(t - t_0) \quad (7)$$

where Φ_0 = notional creep coefficient dependent on relative humidity of ambient environment, mean compressive strength of concrete at age of 28 days, and size of the member; β_c = function describing the development of creep with time after loading; t = age of concrete; t_0 = age of concrete at start of loading.

For the case of the Jamestown-Verrazzano Bridge this expression becomes:

$$\Phi(t, t_0) = 5.5513 \frac{1}{0.1 + t_0^{0.2}} \left[\frac{t - t_0}{364.3 + (t - t_0)} \right]^{0.3} \quad (8)$$

The equation for determining the time-dependent modulus of elasticity according to CEB-FIP MC 90 and considering the local conditions for this bridge, is given as:

$$E_c(t) = (e^{0.25(1-5.3/t^{0.5})})^{0.5} E_c \quad \text{for } t < 28 \text{ days} \quad (9)$$

$$E_c(t) = E_c \quad \text{for } t \geq 28 \text{ days} \quad (10)$$

where $E_c(t)$ is the modulus of elasticity at an age of t days, and E_c is the modulus of elasticity at an age of 28 days.

ANALYSIS PROCEDURE

The main purpose of this study is to estimate bridge strains and stresses and compare the analytical results with field monitored values. The analytical results are complex due to three main reasons: i) the bridge is constructed in segments with each segment being stressed at different times and this construction sequence needs to be considered during the analysis, ii) material behavior and prestress force losses are time-dependent, and iii) there is a change of the structural system from a cantilever structure to a continuous structure when the closure segment is cast. In order to address the segmental construction sequence and the time dependency of material properties, a step-by-step time-dependent analysis method is followed. To account for the time-dependency of the prestressing losses, the rate of creep method is used. Finally, moment redistribution is employed to account for the change in the statical system⁶.

PRESTRESS LOSSES

Prestress losses are divided into instantaneous losses and time-dependent losses. Instantaneous losses include elastic shortening, friction and anchorage set. These take place immediately upon applying the prestressing force. Time-dependent losses are due to relaxation of stressed tendons, shrinkage of concrete, and creep of concrete. The total loss of stress in a tendon is the sum of the total losses due to each source.

The equation for calculating the losses due to relaxation for low relaxation steel in an interval (K,T) is given as follows:

$$\Delta\sigma_{pR}(K,T) = \frac{\sigma_{ps}(K)}{45} \left(\frac{\sigma_{ps}(K)}{f_{py}} - 0.55 \right) \log\left(\frac{T}{K}\right) \quad (11)$$

where $\sigma_{ps}(K)$ = stress in tendon at the beginning of the interval, f_{py} = yield stress of tendon, K = time at beginning of interval in hours, not less than one hour, and T = time at end of interval in hours. The ratio of initial stress in the tendon to its yield stress has to be greater than 0.55 in order to apply Equation 11. If that is not the case, the initial stress is so low that practically no losses due to relaxation occur.

The total loss of prestress due to concrete shrinkage during an interval (K,T) can be determined by:

$$\Delta\sigma_{ps} = E_{ps}s(K,T) \quad (12)$$

where s is the shrinkage strain, and E_{ps} is the modulus of elasticity of the prestressing steel. The shrinkage strain in this study is calculated using the ACI and CEB methods outlined earlier.

The prestress loss due to creep during an interval (K,T) can be calculated as:

$$\Delta\sigma_{pc(K,T)} = \eta_{pK} \sigma_{cgs(K,T)} \Phi_{(K,T)} \quad (13)$$

with $\eta_{pK} = \frac{E_{ps}}{E_c(K)}$ where $\sigma_{cgs}(K)$ is the stress in the concrete at the centroid of the steel at time K due to the prestressing forces and dead load, $E_c(K)$ is the modulus of elasticity of concrete at time K , E_{ps} is the modulus of elasticity of prestressing steel, and $\Phi_{(K,T)}$ is the creep coefficient function. The concrete creep coefficient function as well as the shrinkage strains are here determined according to the ACI and CEB procedures as outlined earlier.

Instantaneous losses of a post-tensioned member are those losses due to elastic shortening, anchorage set, and friction. While time-dependent losses are here calculated for cantilever tendons as well as for the continuity tendons, in this study, the instantaneous losses are only determined for the cantilever tendons. The continuity tendons are stressed from both ends and, hence, less friction losses occur. For simplification, a reduced initial stress is used for the continuity tendons to account for the instantaneous losses.

RATE OF CREEP METHOD

The rate of creep method is based on the assumption that the age of a structure at the time of loading has no influence on the rate of change of creep with time. This leads to parallel creep curves for concrete loaded at different times, Figure 5. Only a single creep curve is required to calculate creep strains caused by any stress history. Under decreasing stress, creep is overestimated, and under increasing stress, it is underestimated due to the rapid decrease of creep with increasing age if a single creep curve is used.

According to the assumption that the age of a structure at the time of loading has no influence on the rate of change of creep with time, the slopes of all the curves at any instant are the same, Figure 5. Therefore the increment of the creep coefficient function during a time interval (T,K) can be calculated as follows:

$$\Phi_{(T,K)} = \Phi_{(T,K_0)} - \Phi_{(K,K_0)} \quad (14)$$

where K_0 = time at initial loading.

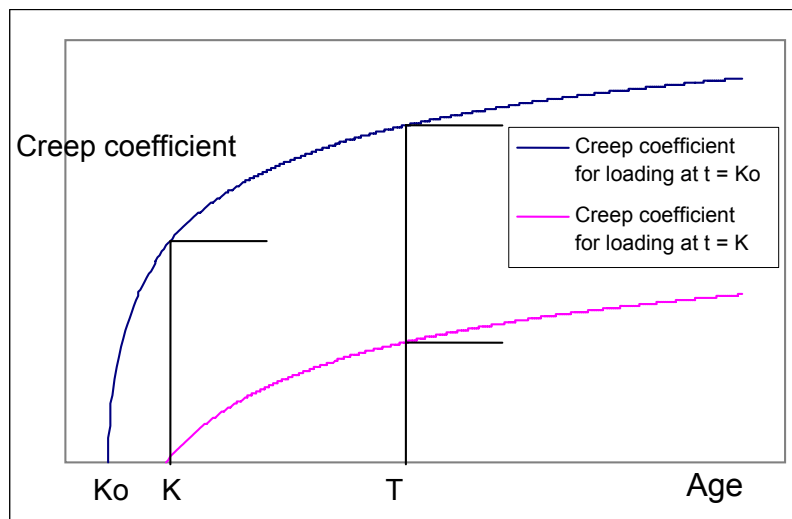


Fig. 5 Creep coefficients according to the rate of creep method

MOMENT REDISTRIBUTION

In this study moment redistribution is accounted for according to the Precast Segmental Box Girder Bridge Manual. Moment redistribution applies to all moments occurring before the bridge is made continuous, i.e. moments due to dead load and those due to cantilever prestressing. Continuity tendons are stressed after bridge completion. Therefore they are not subject to any redistribution.

Moments due to dead load and cantilever prestressing are determined before and after the bridge is made continuous, and the difference δM between these moments is found. For a time interval (K, T) the change in moments can be calculated as follows:

$$M_{c(K,T)} = \delta M [1 - e^{-\Phi(K,T)}] \quad (15)$$

where M_{cr} = creep moment resulting from change of statical system, K=time of completion of closure segment, and $\Phi(K,T)$ = creep coefficient function at the considered location after bridge completion.

RESULTS

CREEP AND SHRINKAGE

In order to compare the final results, it is useful to study first the differences between the creep and shrinkage models used. The theoretical curves used according to ACI and CEB guidelines are compared to creep and shrinkage tests of concrete taken during the construction of the bridge¹. In the case of the creep strains, since the experimental values are given in terms of specific creep, the theoretical creep coefficient functions are divided by the modulus of elasticity of concrete.

Figure 6 shows the specific creep curves for loading at a concrete age of 3 days achieved by the experimental data and the two prediction methods. It can be seen that the specific creep curve determined by the ACI 209 prediction method contains lower values than the curve determined by the CEB MC 90 prediction method as well as the experimentally determined curve. The experimentally determined creep curve almost exactly matches the curve calculated using the CEB MC 90 prediction method.

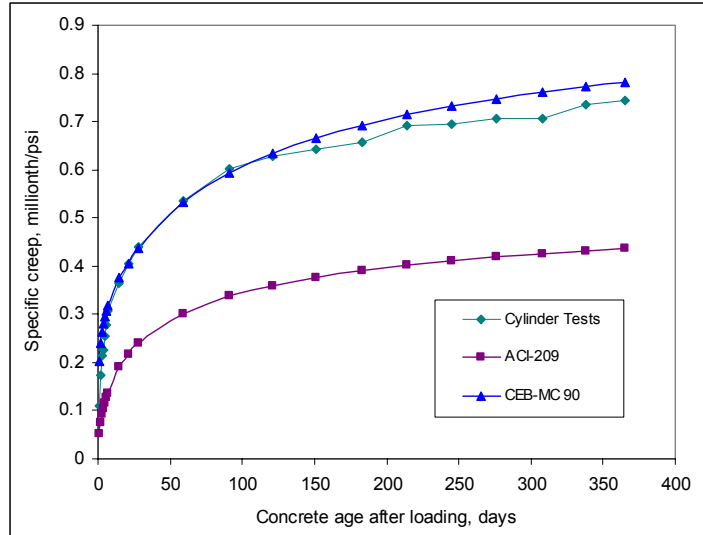


Fig. 6 Concrete Specific Creep for Loading Starting at 3 Days

Shrinkage strains occurring after a concrete age of 3 days are shown in Figure 7. The test data as well as the ACI 209 prediction method provide shrinkage values, which are larger than the ones determined by the CEB MC 90 method. This is due to high shrinkage increments during approximately the first 75 days after the beginning of the test. Afterwards, the slopes of all three curves are similar

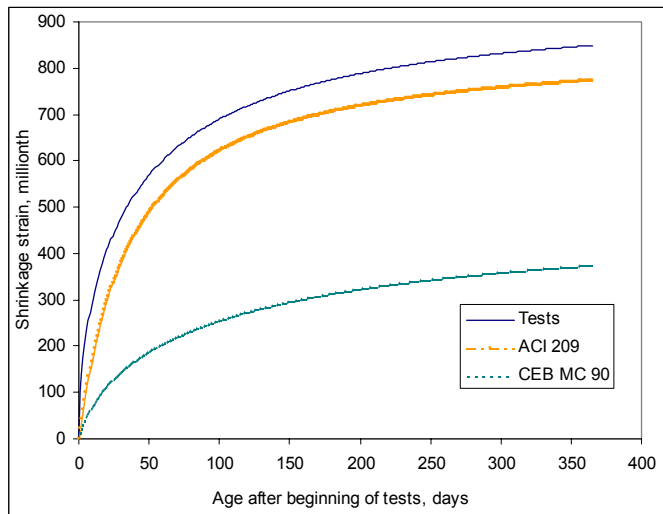


Fig. 7 Concrete Shrinkage Occurring after a Concrete Age of 3 Days

PRESTRESS LOSSES

Prestress losses take place in the cantilever tendons as well as in the continuity tendons. The difference of the forces in the cantilever tendons calculated after losses according to the CEB MC 90 and the ACI 209 prediction methods are small (less than 3%). It can be noted that ACI 209 leads to larger prestress losses in the segments closer to the end of the cantilever than CEB MC 90. Stresses in the segments closer to the end of the cantilever are smaller compared to those closer to the pier. Because of that, prestress losses due to creep have a greater influence on the segments located near the pier while shrinkage losses are larger compared to creep losses at the end of the cantilever. As mentioned the prediction method provided by the CEB MC 90 gives larger creep values than the ACI 209 method, while the latter method leads to larger shrinkage strains.

The total prestress losses, determined according to ACI 209 and CEB MC 90 after 5 years, are similar. The determined value according to ACI 209 equals 2552.34 kips and according to CEB MC 90 it is 2415.27 kips. On the other hand, the sources leading to prestress losses show significant differences in their magnitude, specifically, CEB MC 90 leads to higher creep losses than ACI 209. Based on the CEB MC 90 method, creep losses make up 54% of the total losses, while the shrinkage losses are determined to be 35% of the total losses. According to ACI 209 creep losses of 31% of the total losses and shrinkage losses of 59% of the total losses are calculated. The remaining losses are caused by relaxation of the prestressing steel. Relaxation losses are calculated in the same way for both procedures. They only depend on the initial force at the beginning of every time interval. Differences in relaxation losses are due to different initial forces.

Figure 8 shows the variation of the prestressing force with time in the continuity tendons of the main span closure segment according to CEB MC 90 and ACI 209. It is noted that the slightly lower determined force according to ACI 209 is due to larger prestress losses in the beginning.

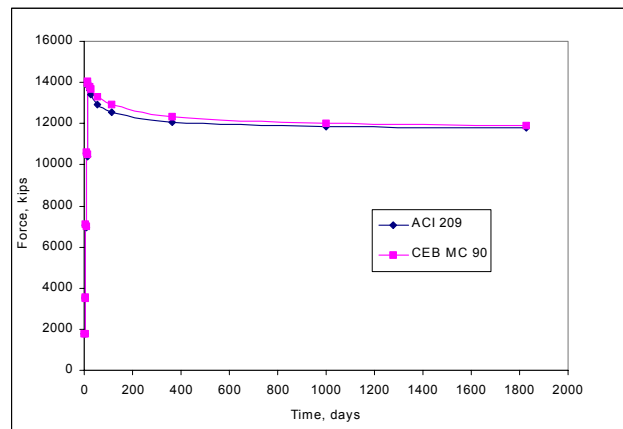


Fig. 8 Prestress Forces in the Continuity Tendons of the Main Closure

STRAINS

A comparison of calculated and measured strains is provided here for the top and bottom slab of the main span closure segment. Figure 9 shows strains in the top slab, and Figure 10 demonstrates those in the bottom slab. Calculated strains are adjusted to the measured strains by considering only those strains, occurring after stressing of the first main span continuity tendons. Shrinkage taking place before stressing of the tendons is subtracted from the total strains.

According to ACI 209 large shrinkage strains are obtained. Better results are achieved using the prediction method provided by the CEB MC 90. For this case the calculated strain curve for the top slab of the main span closure is in good agreement with the strains measured in the top north slab. Strains are slightly underestimated. In the top slab compressive stresses increase with time due to moment redistribution. As mentioned earlier the rate of creep method underestimates strains under increasing stresses.

Calculated strains in the bottom slab according to the CEB MC 90 also indicate a good correlation with the strains measured in the bottom north slab. Measured strains are slightly smaller than calculated strains.

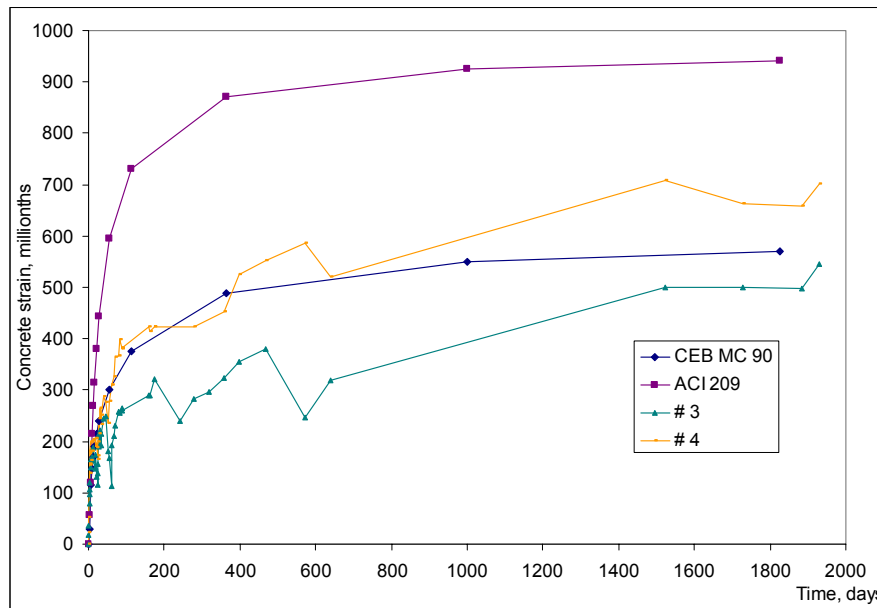


Fig. 9 Predicted and Measured Strains for Top Slab of the Main Closure Segment

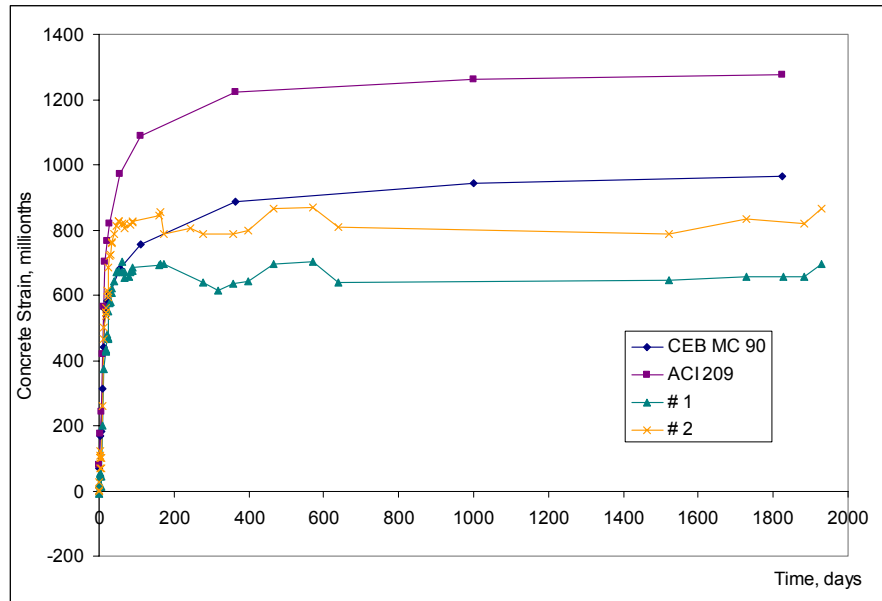


Fig. 10 Predicted and Measured Strains for the Bottom Slab of the Main Closure Segment

CONCLUSIONS

Methods for predicting concrete properties vary significantly. Specific creep estimated using the CEB-FIP MC 90 are in good agreement with the experimentally determined creep curves. On the other hand, using the prediction method provided by the ACI 209 values of specific creep were determined which are smaller than the experimentally determined values. The opposite is true for the case of shrinkage. Shrinkage strains calculated using the CEB MC 90 are smaller than the experimental values which agree much closer with the values calculated using the ACI 209 procedure.

Prestress losses were determined according to the CEB MC 90 and the ACI 209 prediction methods. The time-dependent losses are influenced by the concrete material properties. Therefore larger losses due to creep were calculated using the CEB MC 90 and larger shrinkage losses occurred when the ACI 209 was used. However, the total determined prestress losses were in good agreement using both prediction methods.

Moment redistribution was considered according to the Precast Segmental Concrete Box Girder Bridge Manual. The amount of moment redistribution depends on the creep coefficient functions. Due to that, moment redistribution is larger using the CEB MC 90 than if the creep coefficient is determined according to the ACI 209. Moment redistribution is calculated for moments due to cantilever tendons and dead load. Therefore there is a

redistribution of positive as well as of negative moments. Calculating the total moment due to redistribution by adding the dead load moments and the moments caused by stressing the cantilever tendons, similar results were obtained using both ACI 209 and CEB MC 90.

The calculated strains in the main span closure segment showed large differences. If the concrete properties determined by the ACI 209 are used for the rate of creep method, large strains are calculated. This is due to the large shrinkage strains occurring according to the ACI 209. Using the prediction method provided by the CEB MC 90, smaller strains are determined in the top slab as well as in the bottom slab.

Comparing the measured strains with the calculated ones it can be noted that good results occur if concrete property calculations are performed according to the CEB MC 90. Under decreasing stress the strains are overestimated, and under increasing stress they are underestimated. Calculations according to the ACI 209 considerably overestimated the total strain under increasing as well as under decreasing stresses.

ACKNOWLEDGEMENT

The support of the Rhode Island Department of Transportation is gratefully appreciated. Colin Franco, Francis Manning, Mazen Alsabe, Jan Bak, Joe Boardman, and Lee Perkins from RIDOT provided helpful information including material properties and construction details of the bridge. Installation of the sensors and material testing was done by the Construction Technology Laboratories (CTL).

REFERENCES

1. Weinmann, T.L., and Russel, H.G., "Instrumentation of the Jamestown-Verrazzano Bridge at Jamestown, Rhode Island, *Report*, Construction Technology Laboratories (CTL), Skokie, IL, March 1994.
2. Weinmann, et. al., "Operation Manual for the Datalogger System Installed in the Jamestown-Verrazzano Bridge," *Report*, Construction Technology Laboratories (CTL), Skokie, IL, 1997.
3. Tsiatas, G., and Chen, H., "Monitoring of Long-Term Shrinkage, Creep and Temperature Behavior of the Jamestown-Verrazzano Bridge," *Report*, Civil & Env. Engineering, Univ. of Rhode Island, 1999.
4. American Concrete Institute (ACI) Committee 209, "Prediction of creep, shrinkage, and temperature effects in concrete structures," *Report*, ACI 209R-92, 1992.
5. Comite Euro-International du Beton (CEB), "CEB-FIP Model Code 1990," *Report*, CEB Committee International Bulletin No. 195, 1990.
6. Tsiatas, G., and Essmann, S., "Time Dependent Behavior of the Jamestown-Verrazzano Bridge," *Report URI-ST*, Civil & Env. Engineering, Univ. of Rhode Island, 2000.